

ARTICLE

Received 26 Feb 2014 | Accepted 20 Jun 2014 | Published 24 Jul 2014

DOI: 10.1038/ncomms5481

OPEN

Modest $\text{Ca}_v1.3_{42}$ -selective inhibition by compound **8** is β -subunit dependent

Hua Huang¹, Cheng Yang Ng², Dejie Yu¹, Jing Zhai¹, Yulin Lam² & Tuck Wah Soong^{1,3,4,5}

Two voltage-gated calcium channel subtypes— $\text{Ca}_v1.2$ and $\text{Ca}_v1.3$ —underlie the major L-type Ca^{2+} currents in the mammalian central nervous system. Owing to their high sequence homology, the two channel subtypes share similar pharmacological properties, and at high doses classic calcium channel blockers, such as dihydropyridines, phenylalkylamines and benzothiazepines, do not discriminate between the two channel subtypes. Recent progress in treating Parkinson's disease (PD) was marked by the discovery of synthetic compound **8**, which was reported to be a highly selective inhibitor of the $\text{Ca}_v1.3$ L-type calcium channels (LTCC). However, despite a previously reported IC_{50} of $\sim 24 \mu\text{M}$, in our hands inhibition of the full-length $\text{Ca}_v1.3_{42}$ by compound **8** at $50 \mu\text{M}$ reaches a maximum of 45%. Moreover, we find that the selectivity of compound **8** towards $\text{Ca}_v1.3$ relative to $\text{Ca}_v1.2_{B15}$ channels is greatly influenced by the β -subunit type and its splice isoform variants.

¹Department of Physiology, Yong Loo Lin School of Medicine, National University of Singapore, Singapore 117597, Singapore. ²Department of Chemistry, National University of Singapore, Singapore 117543, Singapore. ³NUS Graduate School for Integrative Sciences and Engineering, Singapore 117456, Singapore. ⁴Neurobiology/Ageing Programme, National University of Singapore, Singapore 117456, Singapore. ⁵National Neuroscience Institute, Jalan Tan Tock Seng, Singapore 308433, Singapore. Correspondence and requests for materials should be addressed to T.W.S. (email: phsstw@nus.edu.sg).

Parkinson's disease (PD) is a movement disorder arising from the degeneration of dopaminergic neurons in the substantia nigra pars compacta (SNc). Although mutations of several genes have been associated with PD¹, 95% of PD cases are idiopathic. The over-reliance of Ca_v1.3 current for pacemaking in the adult SNc neurons was reported to aggravate mitochondrial oxidative stress², and consequently enhance the susceptibility of these neurons towards toxins such as MPTP (1-methyl-4-phenyl-1,2,3,6-tetrahydropyridine) and rotenone³. Significantly, pharmacological blockade or genetic deletion of Ca_v1.3 channels confers protection against toxin induced neuronal damage³. Interestingly, population studies also revealed significant reduction in the risk of developing PD among hypertensive subjects receiving dihydropyridines (DHPs), classical blockers of L-type calcium channels^{4,5}.

Voltage-gated calcium channels Ca_v1.2 and Ca_v1.3 underlie the majority of L-type calcium currents in the central nervous system. While Ca_v1.3 channels contribute only 20% of the total L-type currents in the central nervous system, the use of non-selective DHPs that also inhibits Ca_v1.2 channels could have profound neuro-physiological consequences⁶. In addition, neuronal transcripts of Ca_v1.3 channels display extensive alternative splicing patterns, generating splice variants with different biophysical and pharmacological properties^{7–9}. The Ca_v1.3_{42a} splice variant with a truncated C terminus displayed attenuated sensitivity towards DHP as compared with the long-form Ca_v1.3₄₂ channels⁸. Tissue-selective expression of various Ca_v1.3 splice variants would therefore require different dosages for effective inhibition of the Ca_v1.3 currents.

Recently, Kang *et al.*¹⁰ reported the identification of 1-(3-chlorophenethyl)-3-cyclopentylpyrimidine-2,4,6(1H,3H,5H)-trione, also known as compound **8** as a pharmacological blocker highly selective for Ca_v1.3 (IC₅₀ = 24.3 ± 0.7 μM) over Ca_v1.2 channels. In the current study, we evaluated compound **8** for its activity against different Ca_v1.3 channel splice isoforms. Unexpectedly, initial heterologous expression in human embryonic kidney 293 (HEK293) cells co-transfected with β_{2a}-subunit revealed that compound **8** inhibited Ca_v1.2 more than either Ca_v1.3₄₂ or Ca_v1.3_{42a} channels. Replacing β_{2a}-subunit with β₁-, β₃- or β₄-subunit on the other hand yielded results that showed modest selective inhibition of compound **8** against Ca_v1.3₄₂ over Ca_v1.2_{B15} channels. However, there was clearly no selective inhibition of compound **8** against Ca_v1.3_{42a} and Ca_v1.2 channels in the presence of anyone of the other three β-subunits. Based on the existing data, we conclude that the Ca_v1.3-selective inhibition by compound **8** is modest and is highly dependent on the composition of the Ca_v1.3 splice variant in association with a particular type of β-subunit.

Results

Compound **8** is not selective against Ca_v1.3 with β_{2a}-subunit.

Compounds **1**, **8** and **PYT** (1,3-bis(4-chlorophenethyl)pyrimidine-2,4,6(1H, 3H, 5H)-trione; Fig. 1) were synthesized according to the procedure reported by Kang *et al.*¹⁰ but with slight modifications (see Methods section). It has been reported that the newly discovered compound **8** inhibited ~30 and 60% of Ca_v1.3 current at concentrations of 5 and 50 μM, respectively, whereas Ca_v1.2 channels were weakly responsive as 50 μM of compound **8** inhibited only close to 10% of its peak current¹⁰.

We have recently discovered that alternative splicing at the C terminus regulated the sensitivity of Ca_v1.3 channels towards DHPs; while the long-form Ca_v1.3₄₂ channel exhibited high sensitivity towards DHP; truncation of the C terminus immediately after the IQ domain via alternate use of exon 42a yielded the less sensitive Ca_v1.3_{42a} channel⁸. To determine whether the

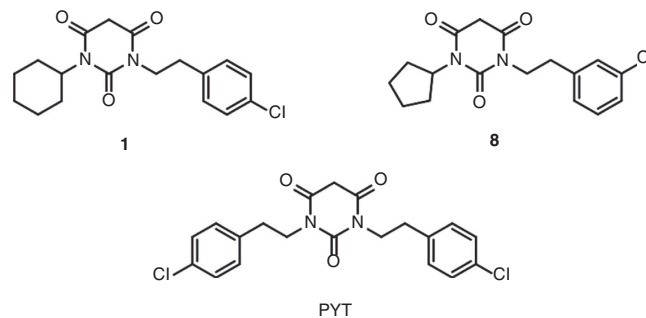


Figure 1 | Structures of compounds **1, **8** and **PYT**.**

compound **8** may also have differential effects on different C-terminal splice forms, we first tested the sensitivity of rat Ca_v1.3₄₂ and Ca_v1.3_{42a}. In the presence of β_{2a} cotransfected with the Ca_v1.3 channels, the channel isoforms displayed very little run-down with repeated 1 s square pulse depolarization to test potential of 10 mV from a holding potential of -70 mV at the frequency of 0.05 Hz (Figs 2b and 3b). Surprisingly, 5 μM of compound **8** failed to significantly inhibit the peak Ca²⁺ current (*I*_{Ca}) of either Ca_v1.3₄₂ or Ca_v1.3_{42a} (Figs 2 and 3) as compared with the untreated controls. Moreover, 50 μM of compound **8** only inhibited 29.51 ± 3.01 and 23.57 ± 2.14% of the peak *I*_{Ca} of Ca_v1.3₄₂ or Ca_v1.3_{42a}, respectively (Figs 2 and 3). In addition, Ca_v1.3₄₂ channels were blocked to a similar level with compound **8** obtained from an additional source (Supplementary Fig. 1). In comparison, 78.85 ± 2.63% of Ca_v1.3₄₂ current and 68.14 ± 3.43% of Ca_v1.3_{42a} current could be robustly inhibited by 5 μM of nimodipine (Figs 2 and 3). As compound **8** has been reported to have little effect on Ca_v1.2 current, we tested its inhibition on the rat Ca_v1.2_{B15} channels¹¹. As compared with the Ca_v1.3, a slightly enhanced run-down effect (10.14 ± 3.98%) was observed for Ca_v1.2_{B15} channels (Fig. 4b). However, 34.97 ± 4.39 and 44.03 ± 4.67% of Ca_v1.2_{B15} current could be inhibited by 5 and 50 μM of compound **8**, respectively, indicating a stronger inhibitory effect of compound **8** on Ca_v1.2 than Ca_v1.3 channels. As expected, 80.66 ± 2.82% of Ca_v1.2_{B15} current was blocked by 5 μM nimodipine (Fig. 4).

In addition, we evaluated the inhibitory activities of **PYT** and compound **1** against Ca_v1.3 and Ca_v1.2 channels¹⁰. Kang *et al.*¹⁰ reported that **PYT** was the original scaffold that displayed an eightfold selectivity for Ca_v1.3, whereas compound **1** was one of the **PYT** analogues that was 28 times more selective for Ca_v1.3 channels. However, in our experiments, 5 μM of **PYT** and compound **1** did not significantly inhibit the peak *I*_{Ca} of Ca_v1.3₄₂ (Supplementary Fig. 2). In addition, 5 μM of **PYT** inhibited 19.90 ± 2.59% of Ca_v1.3_{42a} current, whereas 5 μM of compound **1** had no effect on Ca_v1.3_{42a} channels (Supplementary Fig. 3). In comparison, **PYT** and compound **1** also appeared to be more selective for Ca_v1.2_{B15} showing 43.52 ± 4.83% and 31.69 ± 4.83% inhibition, respectively, (Supplementary Fig. 4). The effect could not be a result of current run-down as little current decay was observed for the untreated Ca_v1.2 current upon prolonged pulses, and the current density of the recorded cells under all treatment groups were not significantly different in the study (Supplementary Fig. 5).

Furthermore, we noted that the use of the original rat Ca_v1.3₄₂ (ref. 12) (Genbank accession no. AF370010) by Kang *et al.*¹⁰ contained three mutations, including G244S, A1104V and V2123A, that have been shown to drastically alter both the biophysical and pharmacological properties of the channel^{9,13,14}. To test whether the use of uncorrected Ca_v1.3₄₂ channel, named here as Ca_v1.3_{42_UC}, could account for the lack of selectivity

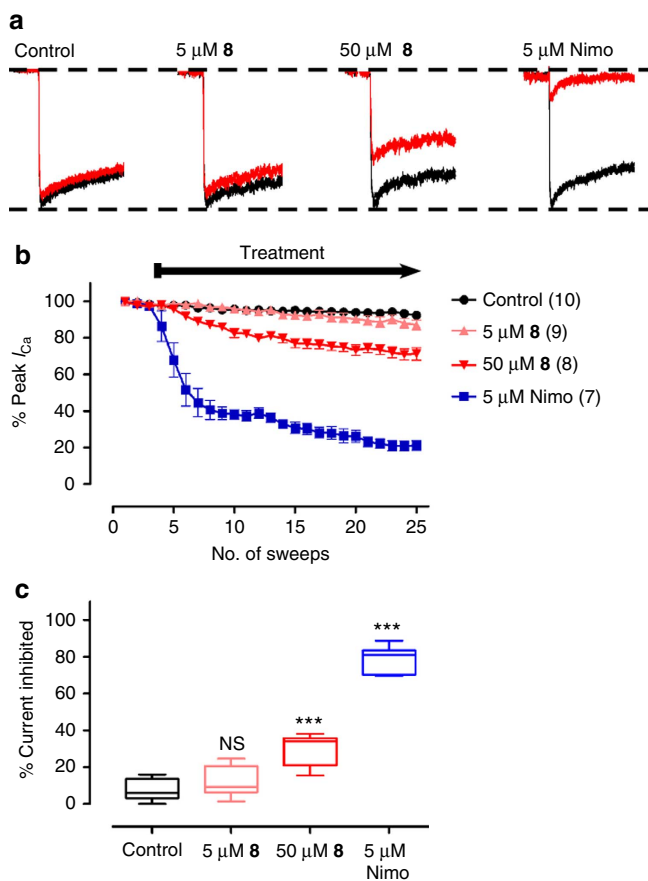


Figure 2 | Inhibition of $\text{Ca}_V1.3_{42}$ current by compound **8 and nimodipine (Nimo).** (a) Representative traces of $\text{Ca}_V1.3_{42}$ currents recorded by single 1 s square pulse to test potential of 10 mV from holding potential of -70 mV for 25 sweeps with sweep interval of 20 s. Only the first three untreated (black) and last three treated (red) traces are shown for each treatment groups. Displayed are the first 100 ms of each recording trace. (b) Averaged diary plot of effects of either control, $5 \mu\text{M}$ **8**, $50 \mu\text{M}$ **8** or $5 \mu\text{M}$ Nimo on $\text{Ca}_V1.3_{42}$ peak currents. The number of cells analysed are indicated in the parenthesis. The drugs were added after the three stable sweeps. (c) Population data of the % peak current inhibition at the 25th sweep normalized against the first sweep conferred by either $5 \mu\text{M}$ **8**, $50 \mu\text{M}$ **8** or $5 \mu\text{M}$ Nimo as compared with the control. NS, non-significant. $***P < 0.001$ (Student's unpaired *t*-test). Alternatively, $P < 0.001$ among all the treatment groups (one-way analysis of variance and Bonferroni's test). The number of cells analysed is indicated in **b**. The data for each condition were collected from two to three transfections.

of compound **8** against $\text{Ca}_V1.3$ channels in the presence of β_2 -subunit, we measured the sensitivity of $\text{Ca}_V1.3_{42_UC}$ to either 5 and $50 \mu\text{M}$ compound **8** or $5 \mu\text{M}$ nimodipine with instead shorter 100 ms depolarizing pulse that was used by Kang *et al.*¹⁰ While $5 \mu\text{M}$ compound **8** has little effect on $\text{Ca}_V1.3_{42_UC}$ channels as compared with control treatment, only $15.75 \pm 3.25\%$ of the peak current could be inhibited by $50 \mu\text{M}$ compound **8**, and expectedly $73.10 \pm 3.48\%$ of the current was blocked by $5 \mu\text{M}$ nimodipine (Fig. 5). Hence, it was consistent that in the presence of β_2 -subunit, $\text{Ca}_V1.2$ displayed higher sensitivity to compound **8** as compared with $\text{Ca}_V1.3$ channels.

β -subunit influences compound **8 selectivity.** Although it has been shown that the presence of different β -subunits did not overtly affect the sensitivity of L-type channels towards DHP¹⁵,

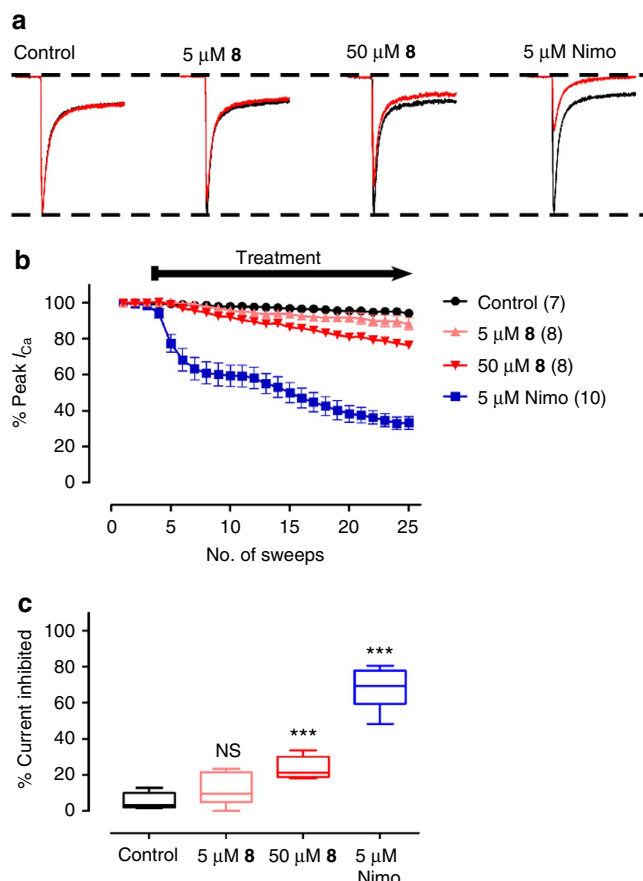


Figure 3 | Inhibition of $\text{Ca}_V1.3_{42a}$ current by compound **8 and nimodipine (Nimo).** (a) Representative traces of $\text{Ca}_V1.3_{42a}$ currents, format as in Fig. 2a. (b) Averaged diary plot of effects either control, $5 \mu\text{M}$ **8**, $50 \mu\text{M}$ **8** or $5 \mu\text{M}$ Nimo on $\text{Ca}_V1.3_{42a}$ peak currents, format as in Fig. 2b. (c) Population data of the % peak current inhibition at the 25th sweep normalized against the first sweep conferred by either $5 \mu\text{M}$ **8**, $50 \mu\text{M}$ **8** or $5 \mu\text{M}$ Nimo as compared with the control. NS, non-significant. $***P < 0.001$ (Student's unpaired *t*-test). Alternatively, $P < 0.001$ among all the treatment groups (one-way analysis of variance and Bonferroni's test). The number of cells analysed is indicated in **b**. The data for each condition were collected from two to three transfections.

the use of different β -subunits such as β_3 in Kang *et al.*¹⁰ and β_2 in the current study might account for the opposite selectivity of compound **8** on $\text{Ca}_V1.2$ and $\text{Ca}_V1.3$ channels observed in these two studies. To test this possibility, we first measured the effect of $50 \mu\text{M}$ compound **8** on $\text{Ca}_V1.3_{42}$, $\text{Ca}_V1.3_{42_UC}$, $\text{Ca}_V1.2_{B15}$ and $\text{Ca}_V1.3_{42a}$ channels co-transfected with β_3 -subunit. Interestingly, while $\sim 40\%$ of the peak I_{Ca} of $\text{Ca}_V1.3_{42}$ and the uncorrected $\text{Ca}_V1.3_{42_UC}$ were similarly inhibited by $50 \mu\text{M}$ compound **8**, $\text{Ca}_V1.2_{B15}$ and $\text{Ca}_V1.3_{42a}$ channels displayed a slightly but significantly weaker sensitivity in comparison with $\text{Ca}_V1.3_{42}$ channels as 23.47 ± 2.60 and $29.05 \pm 2.48\%$ of respective peak currents were inhibited (Fig. 6 and Supplementary Fig. 6). Additional experiments done using either β_1 - and β_4 -subunits produced results that demonstrated enhanced inhibitory effect of compound **8** on $\text{Ca}_V1.3_{42}$ as compared with $\text{Ca}_V1.3_{42_UC}$, $\text{Ca}_V1.2_{B15}$ and $\text{Ca}_V1.3_{42a}$ channels. However, $\text{Ca}_V1.2_{B15}$ and $\text{Ca}_V1.3_{42a}$ channels were inhibited to similar level by $50 \mu\text{M}$ compound **8** in the presence of β_1 -, β_3 - and β_4 -subunits (Fig. 6 and Supplementary Fig. 6). Significantly, in the presence of β_2 , $\text{Ca}_V1.2_{B15}$ still displayed higher sensitivity as compared with $\text{Ca}_V1.3_{42}$, $\text{Ca}_V1.3_{42_UC}$ and $\text{Ca}_V1.3_{42a}$, even when

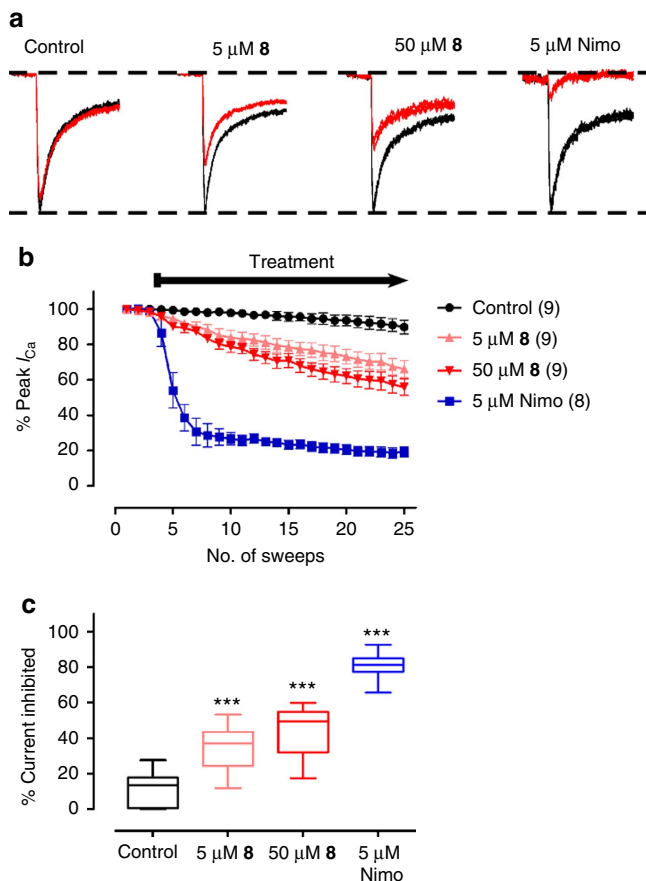


Figure 4 | Inhibition of $\text{Ca}_V1.2_{B15}$ current by compound **8 and nimodipine (Nimo).** (a) Representative traces of $\text{Ca}_V1.2_{B15}$ currents, format as in Fig. 2a. (b) Averaged diary plot of effects of either control, 5 μM **8**, 50 μM **8** or 5 μM Nimo on $\text{Ca}_V1.2_{B15}$ peak currents, format as in Fig. 2b. (c) Population data of the % peak current inhibition at the 25th sweep normalized against the first sweep conferred by either 5 μM **8**, 50 μM **8** or 5 μM Nimo as compared with the control. *** $P < 0.001$. (Student's unpaired t -test) Alternatively, $P < 0.001$ among all the treatment groups (one-way analysis of variance and Bonferroni's test). The number of cells analysed is indicated in b. The data for each condition were collected from two to three transfections.

the currents were repeatedly recorded with a shorter 100-ms depolarizing square pulse (Fig. 6 and Supplementary Fig. 6). Finally, we performed analysis of the correlation of the % of inhibition with the current density for each of the $\text{Ca}_V1.3_{42}$, $\text{Ca}_V1.3_{42_UC}$, $\text{Ca}_V1.2_{B15}$, and $\text{Ca}_V1.3_{42a}$ channels. Only weak correlations were observed as indicated by the following R^2 values: 0.0121 for $\text{Ca}_V1.3_{42}$, 0.0859 for $\text{Ca}_V1.3_{42_UC}$, 0.2439 for $\text{Ca}_V1.2_{B15}$ and 0.2047 for $\text{Ca}_V1.3_{42a}$. Therefore, the inhibitory effect of compound **8** on the $\text{Ca}_V1.2$ and $\text{Ca}_V1.3$ channels are not influenced by the amplitudes of the currents. (Supplementary Fig. 7).

Discussion

PD is a debilitating movement disorder currently with no cure. The constant Ca^{2+} influx via the $\text{Ca}_V1.3$ channels enhances mitochondrial oxidative stress that could contribute towards the pathogenesis of PD. The presence of other possible pacemaking current underlied by hyperpolarization-activated and cyclic nucleotide-gated cation (HCN) channel suggested that it might be feasible to block $\text{Ca}_V1.3$ current without

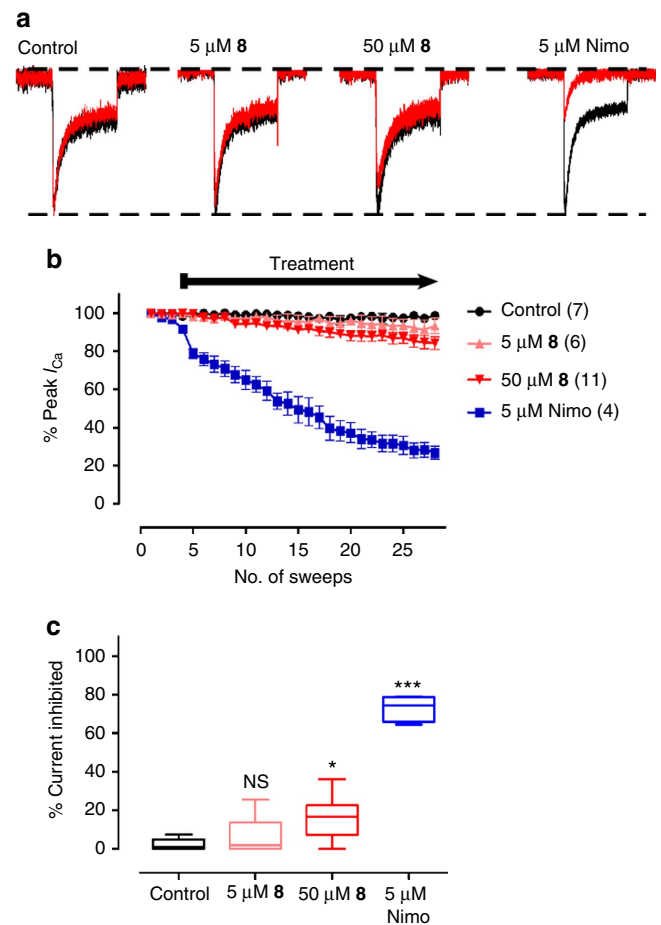


Figure 5 | Inhibition of $\text{Ca}_V1.3_{42_UC}$ current by compound **8 and nimodipine (Nimo).** (a) Representative traces of uncorrected $\text{Ca}_V1.3_{42_UC}$ currents, format as in Fig. 2a. The current was recorded by single square pulse from holding of -70 to 10 mV for over 100 ms with sweep interval of 20 s. (b) Averaged diary plot of effects of either control, 5 μM **8**, 50 μM **8** or 5 μM Nimo on $\text{Ca}_V1.3_{42_UC}$ peak currents, format as in Fig. 2b. (c) Population data of the % peak current inhibition at the 28th sweep normalized against the first sweep conferred by either 5 μM **8**, 50 μM **8** or 5 μM Nimo as compared with the control. * $P < 0.05$, *** $P < 0.001$ (Student's unpaired t -test). Alternatively, $P < 0.001$ among all the treatment groups (one-way analysis of variance and Bonferroni's test). The number of cells analysed is indicated in b. The data for each condition were collected from two to three transfections.

grossly affecting the normal physiological functions of SNC neurons³. The availability of a $\text{Ca}_V1.3$ channel-specific antagonist that could eventually replace non-selective L-type blockers such as DHPs would therefore be ideal for the therapeutic management of PD.

In contrast to the IC_{50} of $24.3 \pm 0.7 \mu\text{M}$ as determined using patch-clamp electrophysiology by Kang *et al.*¹⁰, our initial data with β_2a -subunits revealed that the percentage inhibition of compound **8** on $\text{Ca}_V1.3$ channels at 50 μM was only 30% while at 5 μM no significant inhibition was observed. In contrast to the published report, the inhibition of $\text{Ca}_V1.2$ channels at 50 and 5 μM were 44% and 35%, respectively, indicating selectivity of compound **8** against $\text{Ca}_V1.2$ channels.

The initial failure to observe any selectivity of compound **8** in inhibiting $\text{Ca}_V1.3$ channels led us to investigate the effect of compound **8** with other β -subunits. However, while the $\text{Ca}_V1.3_{42}$ current was indeed more sensitive than $\text{Ca}_V1.2$ in the presence of

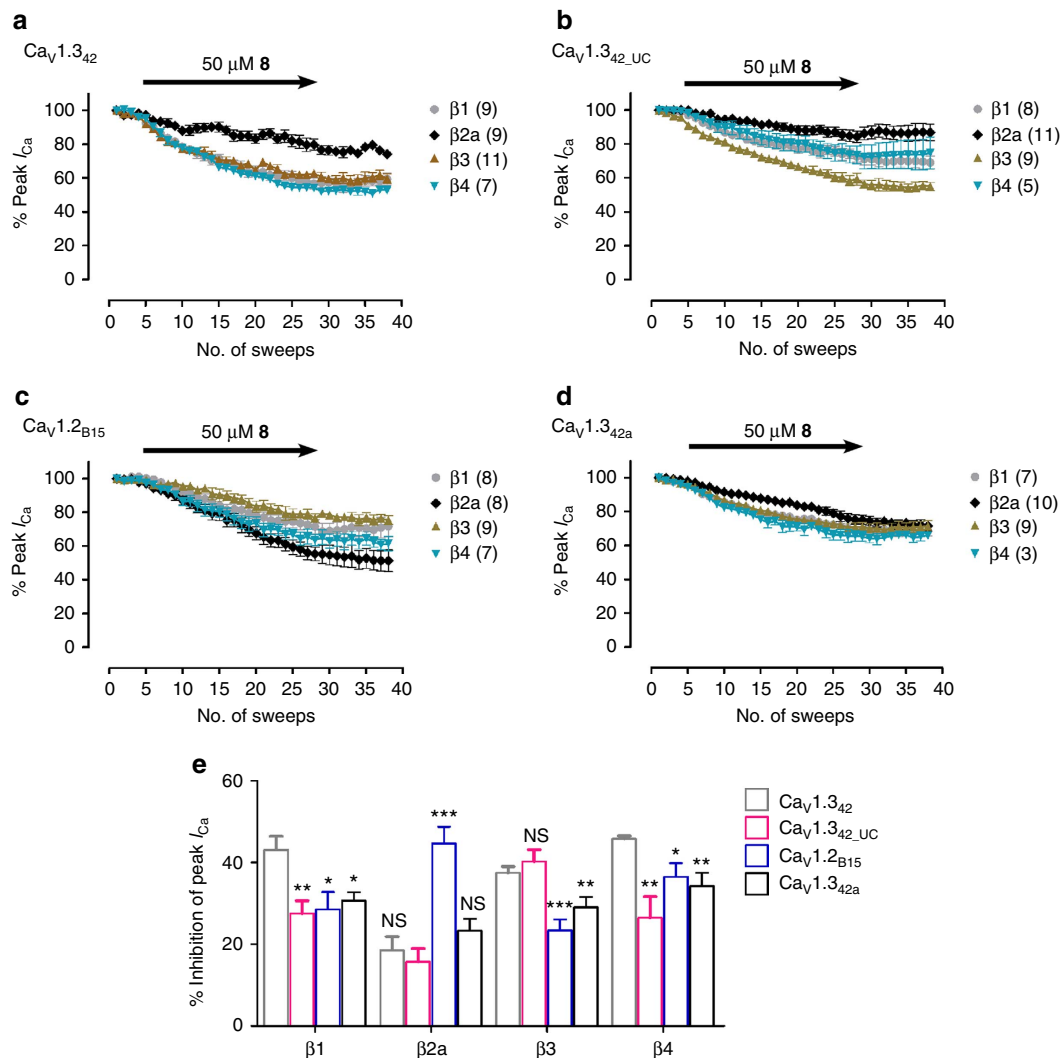


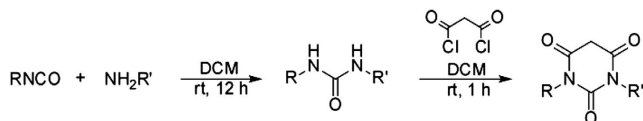
Figure 6 | Inhibition of $Ca_V1.3_{42}$, $Ca_V1.3_{42_UC}$, $Ca_V1.2_{B15}$ and $Ca_V1.3_{42a}$ current by 50 μM compound **8 in the presence of different β -subunits.**

(a) Averaged diary plot of effects of 50 μM **8** on $Ca_V1.3_{42}$ peak currents in the presence of $\beta 1$ -, $\beta 2a$ -, $\beta 3$ - and $\beta 4$ -subunit. The current was recorded by single square pulse from holding of -70 to 10 mV for over 100 ms with sweep interval of 20 s. (b-d) Averaged diary plot of effects of 50 μM **8** on the peak currents of $Ca_V1.3_{42_UC}$, $Ca_V1.2_{B15}$ and $Ca_V1.3_{42a}$, respectively, in the presence of different β -subunits, format as in a. (e) Comparison of the % peak current inhibition at the 28th sweep normalized against the first sweep conferred by 50 μM **8** for $Ca_V1.3_{42}$, $Ca_V1.3_{42_UC}$, $Ca_V1.2_{B15}$, $Ca_V1.3_{42a}$ in the presence of different β -subunits. Within each β -subunit, the % inhibitions of $Ca_V1.3_{42_UC}$, $Ca_V1.2_{B15}$, $Ca_V1.3_{42a}$ were compared with that of $Ca_V1.3_{42}$. NS, non-significant, * $P < 0.05$, ** $P < 0.01$, *** $P < 0.001$ (Student's unpaired *t*-test). Alternatively, $P < 0.001$ within each group (one-way analysis of variance and Bonferroni's test). The number of cells analysed is indicated in b-d. The data for each condition were collected from two to three transfections.

$\beta 1$ -, $\beta 3$ - and $\beta 4$ -subunits, only 35–45% of the its peak currents could be blocked by 50 μM compound **8**, and the percentage of inhibition on $Ca_V1.2_{B15}$ channels was a modest 10–15% less as compared with $Ca_V1.3_{42}$ channels.

To complicate the story further, the short-form $Ca_V1.3_{42a}$ channels displayed similar level of sensitivity as compared with $Ca_V1.2_{B15}$ channels with either $\beta 1$ -, $\beta 3$ - or $\beta 4$ -subunit co-transfected. The $Ca_V1.3_{42a}$ splice variant accounts for $\sim 30\%$ of the total $Ca_V1.3$ transcripts in the substantia nigra region⁷. While the roles of different $Ca_V1.3$ splice variants in neurodegeneration of SNc neurons in the pathogenesis of PD awaits further clarification, the larger current density and more hyperpolarized-shifted I-V relationship implied a greater involvement of $Ca_V1.3_{42a}$ current in driving the pacemaking activity in the SNc neurons as compared with the full-length $Ca_V1.3_{42}$ channels⁸.

In summary, the newly reported compound **8** is not a potent blocker of $Ca_V1.3$ channels as compared with the classical L-type blockers such as the DHPs. The selectivity of compound **8** on $Ca_V1.3_{42}$ over $Ca_V1.2_{B15}$ channels could be influenced strongly by the presence of various β -subunits and the compound **8** was not selective for $Ca_V1.3_{42a}$ over $Ca_V1.2_{B15}$ channels in the presence of $\beta 1$ -, $\beta 3$ - or $\beta 4$ -subunit. Instead, in the presence of $\beta 2a$, compound **8** strongly inhibits $Ca_V1.2_{B15}$ channels over all the $Ca_V1.3$ splice variants tested. Given the differential distribution of β -subunits and the varied expression levels of $Ca_V1.3$ channel variants across various neuronal types, brain regions and organs, the use of compound **8** as a $Ca_V1.3$ -selective antagonist needs to be further clarified. Nonetheless, the quest for discovering a highly selective and potent compound targeting $Ca_V1.3$ channels is a highly worthwhile goal.



Scheme 1 | General synthetic scheme of *N,N'*-disubstituted pyrimidinetrione analogue.

Methods

General synthesis information. All commercially available reagents were bought from Sigma-Aldrich and Alfa Aesar, and used without further purification. Thin layer chromatography was performed using pre-coated plate (Merck silica gel 60, F254) and visualized with ultraviolet (UV) light. Flash column chromatography was carried out on Merck silica gel (230–400 mesh). ^1H and ^{13}C nuclear magnetic resonance (NMR) spectra were recorded on Bruker ACF300 (300 MHz) or AMX 500 (500 MHz) spectrometer at 298 K, respectively. All *J* values are reported in Hz and chemical shift (δ) reported in p.p.m. relative to tetramethylsilane. Abbreviations for signal multiplicities are as follow: singlet (s), doublet (d), triplet (t) and multiplet (m). Mass spectra were determined by electrospray ionization (ESI) on Finnigan TSQ 7000. High-performance liquid chromatography was performed using a Shimadzu LCMS-IT-TOF system with a Phenomenex Luma C18 column (50 \times 3.0 mm, 5 μm) using acetonitrile and 0.1% trifluoroacetic acid in water. The mobile phase has a flow rate of 5 ml min $^{-1}$ with gradient flow of acetonitrile increasing from 5 to 90%. UV/visible detector was set at a wavelength of 254 nm.

General synthetic procedure for compounds 1, 8 and PYT. Compounds 1, 8 and PYT were synthesized according to the procedure reported by Kang *et al.*¹⁰ but with slight modifications (Scheme 1). In brief, a solution of isocyanate (1 mmol) in dichloromethane (10 ml), the respective amine (1 mmol) was added and allowed to stir at room temperature overnight. The mixture was then diluted with dichloromethane (8 ml) and malonyl chloride (1.1 mmol) was added dropwise to the mixture at room temperature under vigorous stirring. Upon reaction completion (monitored by thin layer chromatography), the reaction mixture was concentrated and purified via flash column chromatography using hexane: ethyl acetate(3:1) as eluent to afford the final product. Compounds 1, 8 and PYT were characterized via ^1H and ^{13}C NMR, mass spectrometry (ESI) and melting point determination (Supplementary Figs 8, 9 and 10). The characterization data were comparable to those reported by Kang *et al.*¹⁰ Furthermore, the purity of each compound was determined by HPLC (Supplementary Figs 11 and 12), and the compounds were found to have a purity value of over 98%.

1-(4-chlorophenethyl)-3-cyclohexylpyrimidine-2,4,6(1H,3H,5H)-trione (1). White powder; ^1H NMR spectrum (CDCl_3 , 300 MHz): δ 7.21(d, *J* = 8.4 Hz, 2H), 7.12(d, *J* = 8.4 Hz, 2H), 4.54(m, 1H), 3.99(m, 2H) 3.55(s, 1H), 2.81(m, 2H), 2.17(m, 2H), 1.79(m, 2H), 1.58(m, 3H), 1.32(m, 3H); ^{13}C NMR (CDCl_3 , 75 MHz): δ 164.59, 164.41, 150.92, 136.16, 132.33, 130.13, 128.48, 55.12, 42.50, 40.02, 33.15, 28.88, 26.11, 24.93; melting point: 146.6–147.5 $^\circ\text{C}$ (146–148 $^\circ\text{C}$; ref. 11); HRMS(ESI) calculated for $\text{C}_{18}\text{H}_{21}\text{ClN}_2\text{O}_3[\text{M}-\text{H}]^-$: 347.1168; found, 347.1168.

1-(3-chlorophenethyl)-3-cyclopentylpyrimidine-2,4,6(1H, 3H, 5H)-trione (8). White solid; ^1H NMR spectrum (CDCl_3 , 500 MHz): δ 7.23-7.18(m, 3H), 7.12(d, *J* = 4.14 Hz, 1H), 5.12(m, 1H), 4.05(m, 2H), 3.60(s, 2H), 2.86(m, 2H), 1.92(m, 4H), 1.84(m, 2H), 1.57(m, 2H); ^{13}C NMR spectrum (CDCl_3 , 125 MHz): δ 164.68, 164.40, 150.79, 139.77, 134.18, 129.72, 128.96, 127.03, 126.81, 54.24, 42.48, 40.00, 33.55, 28.59, 25.42; melting point: 131.3–131.8 $^\circ\text{C}$ (131–132 $^\circ\text{C}$; ref. 11); HRMS(ESI) calculated for $\text{C}_{17}\text{H}_{19}\text{ClN}_2\text{O}_3[\text{M}-\text{H}]^-$: 333.1011; found, 333.1007.

1,3-bis(4-chlorophenethyl)pyrimidine-2,4,6(1H, 3H, 5H)-trione (PYT). White powder; ^1H NMR (CDCl_3 , 500 MHz): δ 7.28(d, *J* = 8.15 Hz, 4H), 7.17(d, *J* = 8.1 Hz, 4H), 4.06(t, *J* = 7.7 Hz, 4H), 3.60(s, 2H) 2.84(t, *J* = 7.95 Hz, 4H); ^{13}C NMR (CDCl_3 , 125 MHz): δ 164.18, 150.98, 136.07, 132.57, 130.23, 128.67, 42.77, 39.46, 33.26; melting point: 171.8–172.9 $^\circ\text{C}$; HRMS(ESI) calculated for $\text{C}_{20}\text{H}_{18}\text{Cl}_2\text{N}_2\text{O}_3[\text{M}-\text{H}]^-$: 403.0622; found, 403.0612.

Electrophysiological recordings and data analysis. Whole-cell patch-clamp electrophysiological recordings were used to characterize the recombinant rat $\text{Ca}_v1.3_{42}$ and of $\text{Ca}_v1.3_{42a}$ channels⁸, and rat $\text{Ca}_v1.2_{B15}$ channel⁹. I_{Ca} currents were recorded from transiently transfected mammalian HEK293 cells at room temperature with calcium phosphate method^{16,17}. Outward I_{Ca} currents were blocked by Cs^+ in the internal and external solutions. Cells were transiently transfected with the respective $\text{Ca}_v1.3$ and $\text{Ca}_v1.2$ constructs with rat β_{2a} -subunit and rat $\alpha_2\delta$ -subunit using standard calcium phosphate transfection method. For whole-cell patch-clamp recording, the internal solution (patch-pipette solution) contained the following (in mM): 138 Cs-MeSO₃, 5 CsCl, 5.0 EGTA, 10 HEPES and 1 MgCl₂, and 2 mg ml $^{-1}$ Mg-ATP, pH 7.3 (adjusted with CsOH), and

290 mOsm with glucose. The external solution contained the following (in mM): 109 NaCl, 10 CaCl₂, 1 MgCl₂, 20 CsCl and 10 HEPES, (pH adjusted to 7.4 with CsOH and osmolality to 290 glucose). Pipettes of resistance 1.5–2 M Ω were used. Whole-cell currents, obtained under voltage clamp with an Axopatch 200B amplifier (Molecular Devices, Union City, CA), were filtered at 1–5 kHz and sampled at 5–50 kHz, and the series resistance was typically <5 M Ω after >80% compensation. A P/4 protocol was used to subtract on-line the leak and capacitive transients.

The currents were recorded by single square pulse from holding of -70 to 10 mV for over 1 s or 100 ms with sweep interval of 20 s. Data were acquired using the software pClamp9 (Molecular Devices), and analysed and fitted using GraphPad Prism V software (San Diego, CA) and Microsoft (Seattle, WA) Excel. Data are expressed as mean values \pm s.e.m.

Drug preparation. Stock solutions were prepared by dissolving compound PYT, 1, 8 and nimodipine (RBI) in DMSO to make a 100-mM stock solution and stored at -20 $^\circ\text{C}$ in the dark. Respective concentrations were freshly prepared in the bath solution from stock, and perfused (1 ml per min) into the whole recording chamber by gravity during current recording. The cell selected for patch-clamp recording were positioned as close to the outlet as possible. The external solutions were protected from light throughout the experiment.

References

- Lesage, S. & Brice, A. Parkinson's disease: from monogenic forms to genetic susceptibility factors. *Hum. Mol. Genet.* **18**, R48–R59 (2009).
- Guzman, J. N. *et al.* Oxidant stress evoked by pacemaking in dopaminergic neurons is attenuated by DJ-1. *Nature* **468**, 696–700 (2010).
- Chan, C. S. *et al.* 'Rejuvenation' protects neurons in mouse models of Parkinson's disease. *Nature* **447**, 1081–1086 (2007).
- Ascherio, A. & Tanner, C. M. Use of antihypertensives and the risk of Parkinson disease. *Neurology* **72**, 578–579 (2009).
- Ritz, B. *et al.* L-type calcium channel blockers and Parkinson disease in Denmark. *Ann. Neurol.* **67**, 600–606 (2010).
- Sinnesger-Brauns, M. J. *et al.* Isoform-specific regulation of mood behavior and pancreatic beta cell and cardiovascular function by L-type Ca²⁺ channels. *J. Clin. Invest.* **113**, 1430–1439 (2004).
- Bock, G. *et al.* Functional properties of a newly identified C-terminal splice variant of Cav1.3 L-type Ca²⁺ channels. *J. Biol. Chem.* **286**, 42736–42748 (2011).
- Huang, H., Yu, D. & Soong, T. W. C-terminal alternative splicing of Cav1.3 channels distinctively modulates their dihydropyridine sensitivity. *Mol. Pharmacol.* **84**, 643–653 (2013).
- Tan, B. Z. *et al.* Functional characterization of alternative splicing in the C terminus of L-type CaV1.3 channels. *J. Biol. Chem.* **286**, 42725–42735 (2011).
- Kang, S. *et al.* CaV1.3-selective L-type calcium channel antagonists as potential new therapeutics for Parkinson's disease. *Nat. Commun.* **3**, 1146 (2012).
- Tang, Z. Z., Hong, X., Wang, J. & Soong, T. W. Signature combinatorial splicing profiles of rat cardiac- and smooth-muscle Cav1.2 channels with distinct biophysical properties. *Cell Calcium* **41**, 417–428 (2007).
- Xu, W. & Lipscombe, D. Neuronal Ca(V)1.3 α (1) L-type channels activate at relatively hyperpolarized membrane potentials and are incompletely inhibited by dihydropyridines. *J. Neurosci.* **21**, 5944–5951 (2001).
- Huang, H. *et al.* RNA editing of the IQ domain in Ca(v)1.3 channels modulates their Ca²⁺(+)-dependent inactivation. *Neuron* **73**, 304–316 (2012).
- Lieb, A., Scharinger, A., Sartori, S., Sinnesger-Brauns, M. J. & Striessnig, J. Structural determinants of Cav1.3 L-type calcium channel gating. *Channels (Austin)* **6**, 197–205 (2012).
- Berjukow, S., Marksteiner, R., Gapp, F., Sinnesger, M. J. & Hering, S. Molecular mechanism of calcium channel block by isradipine. Role of a drug-induced inactivated channel conformation. *J. Biol. Chem.* **275**, 22114–22120 (2000).
- Patil, P. G., Brody, D. L. & Yue, D. T. Preferential closed-state inactivation of neuronal calcium channels. *Neuron* **20**, 1027–1038 (1998).
- Peterson, B. Z., DeMaria, C. D., Adelman, J. P. & Yue, D. T. Calmodulin is the Ca²⁺ sensor for Ca²⁺-dependent inactivation of L-type calcium channels. *Neuron* **22**, 549–558 (1999).

Acknowledgements

We would like to thank Dr Joerg Striessnig (Medical School, University of Innsbruck, Austria) for the additional source of compound 8. The work is supported by Singapore Biomedical Research Council and the National Medical Research Council.

Author contributions

H.H. designed and performed the patch-clamp experiments and wrote the initial draft of the manuscript; C.Y.N. synthesized all compounds; Y.D. and J.Z. participated in the

patch-clamp experiment; and Y.L. and T.W.S supervised the experiments and edited the manuscript.

Additional information

Supplementary Information accompanies this paper at <http://www.nature.com/naturecommunications>

Competing financial interests: The authors declare no competing financial interests.

Reprints and permission information is available online at <http://npg.nature.com/reprintsandpermissions/>

How to cite this article: Huang, H. *et al.* Modest $\text{Ca}_v1.3_{42}$ -selective inhibition by compound **8** is β -subunit dependent. *Nat. Commun.* 5:4481 doi: 10.1038/ncomms5481 (2014).



This work is licensed under a Creative Commons Attribution-NonCommercial-ShareAlike 4.0 International License. The images or other third party material in this article are included in the article's Creative Commons license, unless indicated otherwise in the credit line; if the material is not included under the Creative Commons license, users will need to obtain permission from the license holder to reproduce the material. To view a copy of this license, visit <http://creativecommons.org/licenses/by-nc-sa/4.0/>